PERGAMON

Polyhedron 20 (2001) 1139–1145

POLYHEDRON

www.elsevier.nl/locate/poly

Single-molecule magnets: Jahn–Teller isomerism and the origin of two magnetization relaxation processes in Mn_{12} complexes

Sheila M.J. Aubin [a], Ziming Sun [a], Hilary J. Eppley [b], Evan M. Rumberger [a], Ilia A. Guzei [c], Kirsten Folting [b], Peter K. Gantzel [a], Arnold L. Rheingold [c], George Christou* [b,1], David N. Hendrickson* [a,2]

[a] *Department of Chemistry and Biochemistry-0358, University of California at San Diego, La Jolla, CA 92093, USA*
[b] *Department of Chemistry and Molecular Structure Center, Indiana University, Bloomington, IN 47405-4001, USA*
[c] *Department of Chemistry and Biochemistry, University of Delaware, Newark, DE 19716, USA*

Received 17 September 2000; accepted 28 October 2000

Abstract

Different crystallographic forms of the single molecule magnet $[Mn_{12}O_{12}(O_2CR)_{16}(H_2O)_4]$ with a given R substituent have been isolated. X-ray structures are reported for two isomeric forms of the *p*-methylbenzoate complex, $[Mn_{12}O_{12}(O_2CC_6H_4$-*p*-$Me)_{16}(H_2O)_4]\cdot(HO_2CC_6H_4$-*p*-Me) (**2**) and $[Mn_{12}O_{12}(O_2CC_6H_4$-*p*-$Me)_{16}(H_2O)_4]\cdot 3H_2O$ (**3**). The Mn_{12} molecules in complexes **2** and **3** are geometrical isomers differing in the positions of the H_2O and carboxylate ligands. In complex **2**, one Mn^{III} ion has an abnormal Jahn–Teller distortion axis oriented at an oxide ion, and thus **2** and **3** are also Jahn–Teller isomers. This reduces the symmetry of the core of complex **2** compared with that of complex **3**. Complex **2** likely has a larger tunneling matrix element and this explains why this complex shows an out-of-phase ac peak (χ''_M) in the signal in the 2–3 K region, whereas complex **3** has its χ''_M peak in the 4–7 K range, i.e. the rate of tunneling of magnetization is greater in complex **2** than complex **3**.

Keywords: Nanomagnets; Magnetization tunneling; Single-molecule magnets

1. Introduction

Individual molecules that function as nanomagnets have been termed single-molecule magnets (SMMs) [1–38]. The magnetic properties of SMMs are a function of individual molecules and do not result from interactions between molecules in a crystal. Each molecule possesses enough spin and magnetoanisotropy to function as a magnet. At low enough temperatures, each molecule behaves as a single magnetic domain. If an external field is applied, a SMM may be magnetized, with its spin oriented in either an 'up' or 'down' direction along its axial magnetoanisotropy axis. If the temperature is low enough, a SMM will exhibit slow magnetization relaxation phenomena, such as magnetization hysteresis loops and the presence of an out-of-phase ac susceptibility signal. The most thoroughly studied SMM is $[Mn_{12}O_{12}(O_2CMe)_{16}(H_2O)_4]\cdot 2(HO_2$-$CMe)\cdot 4(H_2O)$ (complex **1**).

In order for a molecule to be a SMM it must have a large-spin ground state (S) as well as possess a large *negative* magnetoanisotropy as gauged by the axial zero-field splitting parameter D. Both of these properties contribute to the barrier height of magnetization reversal that scales as $S^2|D|$. Complex **1** has been found to have a $S = 10$ ground state and significant *negative* magnetic anisotropy ($D = -0.50$ cm^{-1}). In zero applied field there are two equivalent lowest energy states corresponding to $m_s = -10$ and $m_s = 10$ and the highest energy state corresponds to $m_s = 0$ (Fig. 1). The height of the potential energy barrier is $|D|S^2 = 50$ cm^{-1}. In order for the magnetic moment of a Mn_{12} molecule to flip from 'up' to 'down' it must either climb over the potential energy barrier in a thermally activated process or pass through the barrier by quantum tunneling.

[1] *Corresponding author.
[2] *Corresponding author. E-mail: dhendrickson@ucsd.edu

0277-5387/01/$ - see front matter
PII: S0277-5387(01)00585-X

A diagnostic technique for observing slow magnetization relaxation of a SMM is ac magnetic susceptibility. A species that possesses a magnetization relaxation mechanism that is slower than the oscillating field produced by the magnetometer cannot stay in phase with this field, and will exhibit a peak in the out-of-phase component of the ac susceptibility. This peak corresponds to a rate in which the magnetic moment of the SMM 'flips' close to the rate of the operating frequency of the instrument. On the other hand, a simple paramagnet will *not* produce a peak in the out-of-phase component of the ac susceptibility, since the rate of the 'flipping' of the magnetic moment of such a species ($\sim 10^9$ Hz) occurs well above the typical (1–1500 Hz) operating frequencies of an ac magnetometer. The origin of the out-of-phase peak observed for complex **1** has been the focus of considerable research [5]. One frequency-dependent peak is observed for the complex **1** in the 4–7 K region. A puzzling observation [9] for several Mn_{12} type molecules is that they may display two, instead of one, frequency dependent peaks in the out-of-phase ac susceptibility response. These peaks often occur in the 2–3 K (low temperature) and 4–7 K (high temperature) ranges. When $kT < |D|m_s^2$, the rate at which the magnetic moment of a molecule flips becomes sluggish and this relaxation phenomenon appears as an out-of-phase ac susceptibility peak within a certain range of frequencies. This leads to one out-of-phase ac signal per Mn_{12} molecule or for a collection of identical Mn_{12} molecules. However, it does *not* explain why a given complex would exhibit two out-of-phase ac signals.

In this report, two new Mn_{12} SMMs are characterized by several techniques including single-crystal X-ray structures. These complexes are geometrical isomers, differing by the ligation of H_2O molecules as well as exhibiting the recently discovered 'Jahn–Teller isomerism' [38]. One complex exhibits a frequency-dependent high-temperature out-of-phase ac susceptibility signal and the other a low-temperature frequency-dependent ac susceptibility signal. An explanation of the difference in ac susceptibility response for these two Mn_{12} isomeric SMMs is given.

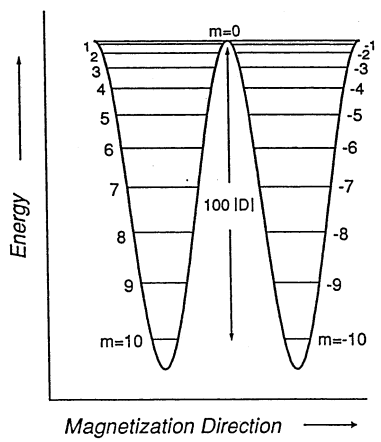

Fig. 1. Plot of potential energy vs. magnetization direction for a single Mn_{12} molecule in zero applied field with a $S = 10$ ground state experiencing a zero-field splitting of $H = D\hat{S}_z^2$, where $D < 0$.

2. Experimental

2.1. Compound preparation

All chemicals and solvents were used as received. All preparations and manipulations were performed under aerobic conditions. $(NBu^n_4)[MnO_4]$ was prepared as previously described [39]. *WARNING*: Organic permanganates should be handled with extreme caution. Detonation of some organic permanganates have been reported while drying at high temperatures.

2.1.1. $[Mn_{12}O_{12}(O_2CC_6H_4\text{-}p\text{-}Me)_{16}(H_2O)_4]\cdot HO_2CC_6H_4\text{-}p\text{-}Me$ (complex **2**)

$Mn(ClO_4)_2$ (4.00 g, 11.0 mmol) was dissolved in 100% ethanol (20 ml) followed by the addition of *p*-methylbenzoic acid (19.13 g, 140.5 mmol) and additional ethanol (180 ml). Solid $(NBu^n_4)[MnO_4]$ (1.55 g, 4.28 mmol) was slowly added followed by filtration. The reddish–brown filtrate was left uncapped and undisturbed for 2 weeks. The resulting brown solid $[Mn_{12}O_{12}(O_2CC_6H_4\text{-}p\text{-}Me)_{16}(H_2O)_4]$ (7% yield based on Mn) was collected on a frit, washed with 100% ethanol, and recrystallized from CH_2Cl_2 hexanes, yielding black needles. Later it was discovered that higher yields (20%) were obtained if the synthesis was done in 2% H_2O:98% ethanol. The resulting microcrystals were washed with 100% ethanol and dried under vacuum. Recrystalization from anhydrous CH_2Cl_2: hexanes lead to black microcrystals. *Anal.* Calc. for $C_{136}H_{128}O_{50}Mn_{12}$: C, 50.70; H, 4.00. Found for $C_{136}H_{128}O_{50}Mn_{12}$: C, 50.78; H, 3.94%.

2.1.2. $[Mn_{12}O_{12}(O_2CC_6H_4\text{-}p\text{-}Me)_{16}(H_2O)_4]\cdot 3H_2O$ (complex **3**)

This complex was prepared in an analogous fashion as for complex **2** except instead of 100% ethanol, a 20% H_2O/80% ethanol solution (260 ml) was used. The yield based on total available Mn was 9%. *Anal.* Calc. for $C_{130}H_{132}O_{54}Mn_{12}$: C, 49.0; H, 4.04. Found for $C_{130}H_{132}O_{54}Mn_{12}$: C, 48.9; H, 4.12%.

2.2. Physical measurements

Alternating current (ac) magnetic susceptibility measurements were collected on an MPMS2 Quantum Design SQUID magnetometer equipped with 1T magnet and capable of achieving temperatures of 1.7–400 K.

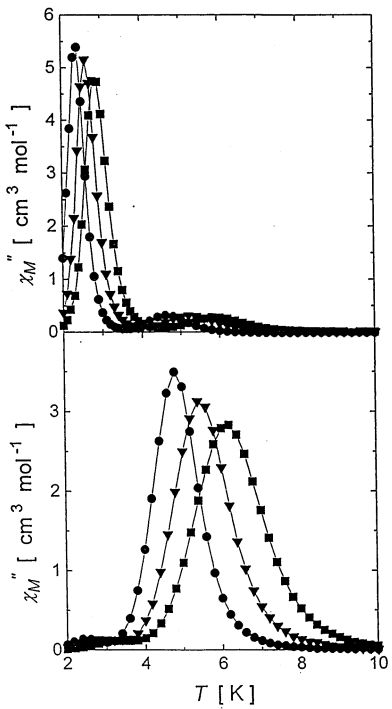

Fig. 2. Plots of χ''_M vs. temperature for the *p*-methylbenzoate complexes **2** (upper) and **3** (lower) in an ac field of 1 G oscillating at 50 Hz (●), 250 Hz (▼) or 1000 Hz (■).

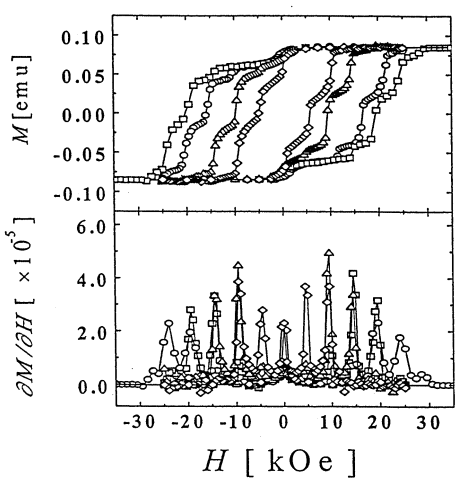

Fig. 3. Plots of magnetization vs. external magnetic field for $[Mn_{12}O_{12}(O_2CC_6H_4\text{-}p\text{-}Me)_{16}(H_2O)_4]\cdot 3H_2O$ (complex **3**) at five temperatures in the 1.72–2.50 K range. Five small crystals (1.2 mg) were oriented in a frozen eicosane matrix so that the magnetic field is parallel to the principal axis of magnetization.

The ac field range is 1×10^{-4} to 5 G, oscillating in a frequency range of 5×10^{-4} to 1512 Hz. Pascal's constants [40] were used to approximate the diamagnetic molar susceptibility contribution for each complex and were subtracted from the experimental molar susceptibility data to give the paramagnetic molar susceptibility data. Ac magnetic susceptibility data were collected on microcrystalline and frozen solution samples in an ac field of 1G, oscillating at frequencies of 50, 250 or 1000 Hz and a dc field of 0 G. Oriented samples of complexes **2** and **3** for magnetization hysteresis measurements were prepared by suspending a few small crystals of either complex in fluid eicosane in the 312–318 K range. In the presence of a 5.5 T magnetic field each crystallite orients with its principal axis of magnetization parallel to the direction of the external field. The eicosane is then cooled to room temperature and this gives a wax cube with the few crystallites magnetically oriented inside. The sweep rate for all hysteresis measurements was 25 Oe s^{-1}.

3. Results and discussion

3.1. Alternating current magnetic susceptibility

In Fig. 2 χ''_M versus T is plotted for complexes **2** (upper) and **3** (lower) in the temperature range of 2–10 K at frequencies of 50, 250 or 1000 Hz. These two crystallographically different forms of the *p*-methylbenzoate Mn_{12} complex each have two frequency-dependent out-of-phase ac peaks, one in the 2–3 K region and the other in the 4–7 K region. However, complex **2** has predominantly one peak in the 2–3 K region, whereas complex **3** (lower trace) has predominantly one peak in the 4–7 K region. It is clear that one crystallographically different form exhibits the lower temperature out-of-phase ac signal, whereas the higher temperature ac peak is attributable to the other crystallographic form.

3.2. Magnetization hysteresis loops

Fig. 3 shows the magnetization hysteresis data measured for complex **3**. Magnetization hysteresis loops are seen in the 1.72–2.50 K range. The coercive magnetic field and consequently the area enclosed within a hysteresis loop increase as the temperature is decreased. Magnetization hysteresis loops were also measured for complex **2** at the temperatures of 1.72, 2.20, 2.00, 1.90 and 1.80 K (Fig. 4). The hysteresis loops for complex **2** are dramatically different than those for complex **3**. When the external field is reduced from +3.5 T to zero, the magnetization falls off dramatically, and the coercive fields are considerably less for complex **2** than for complex **3**. Complex **2** has an appreciably greater rate of magnetization relaxation than does isomeric complex **3**. Thus, these two *p*-methylbenzoate Mn_{12} complexes experience quite different kinetic barriers for reversal of magnetization.

Steps are seen at regular intervals of the external field for both complex **2** and complex **3**. These steps are due to tunneling of the magnetization [20–23]. First deriva-

tive plots were calculated for each of the hysteresis loops (lower plots in Figs. 3 and 4) to clearly show the intervals of the steps.

The magnetization relaxation rates can be quantified by analyzing the frequency dependencies of the χ''_M signals for the two complexes as shown in Fig. 2. Ac susceptibility data were collected at eight different frequencies from 1.0 to 1512 Hz for complex **3**. From the peaks in the χ''_M versus temperature plots, values of the magnetization relaxation time τ were determined at each temperature. The data were least-squares fit to the Arrhenius Eq. (1) to give the values of $\tau_0 = 7.7 \times 10^{-9}$ s and $U_{eff} = 64$ K:

$$\tau = \tau_0 \exp(U_{eff}/kT) \quad (1)$$

A similar analysis of the frequency dependence of the dominant low temperature χ''_M peak in the ac data for complex **2** gives $\tau_0 = 2.0 \times 10^{-10}$ s and $U_{eff} = 38$ K. The activation energy (U_{eff}) for reversal of the direction of the magnetization for complex **2** ($U_{eff} = 38$ K) is considerably less than that ($U_{eff} = 64$ K) for the isomeric complex **3**. The Mn_{12}–acetate complex **1** has been reported [6,7] to have a U_{eff} value of 62 K, very close to the value for complex **3**.

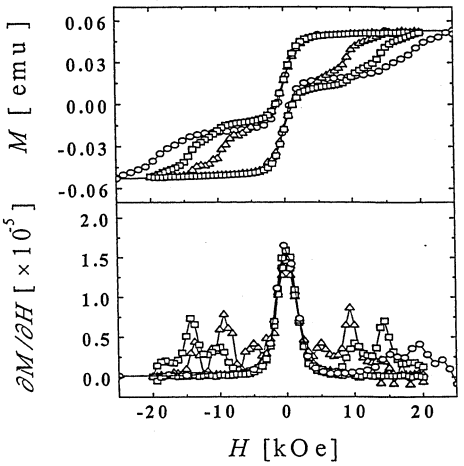

Fig. 4. Plots of magnetization vs. external magnetic field for $[Mn_{12}O_{12}(O_2CC_6H_4\text{-}p\text{-}Me)_{16}(H_2O)_4]\cdot(HO_2CC_6H_4\text{-}p\text{-}Me)$ (complex **2**) at five temperatures in the 1.72–2.20 K range. Six small crystals (2.2 mg) were oriented in a frozen eicosane matrix so that the magnetic field is parallel to the principal axis of magnetization.

Table 1
Crystallographic data for complexes **2** and **3**

Parameter	Complex **3**	Complex **2**
Formula	$C_{128}H_{126}Mn_{12}O_{51}$	$C_{136}H_{128}Mn_{12}O_{50}$
Formula weight (g mol^{-1}) [a]	3139.46	3221.66
Space group	*I*2/*a*	*C*2/*c*
Unit cell dimensions		
a (Å)	29.2794(4)	40.4589(5)
b (Å)	32.3271(4)	18.2288(2)
c (Å)	29.8738(6)	26.5882(4)
α (°)	90	90
β (°)	99.2650(10)	125.8359(2)
V (Å^3)	27907.2(8)	15897.1(4)
Z	8	4
Crystal color, habit	black block	black block
D_{calc} (g cm^{-3})	1.488	1.346
μ(Mo Kα) (cm^{-1})	11.31	9.94
Temperature (K)	223(2)	193(2)
Absorption correction	empirical	empirical
T_{max}/T_{min}	1.000/0.390	1.000/0.382
Diffractometer	Siemens P4/CCD	
Radiation	Mo Kα ($\lambda = 0.71071$ Å)	
$R(F)$% [a]	8.80	10.21
$R(wF^2)$ (%) [a]	21.58	24.88

[a] Quantity minimized $= R(wF^2) = \Sigma[w(|F_o|^2 - |F_c|^2)^2/\Sigma[(wF_o^2)^2]^{1/2}$; $R = \Sigma(||F_o| - |F_c||)/\Sigma|F_o|$.

3.3. X-ray structures of the p-methylbenzoate complexes 2 and 3

As is clear from Table 1, complexes **2** and **3** are crystallographically different. Complex **2** crystallizes in the *C*2/*c* space group and has one molecule of *p*-methylbenzoic acid as a solvate molecule. This solvate molecule was found to be disordered in the refinement of the X-ray data. Complex **3** crystallizes in the *I*2/*a* space group. In the refinement **3**, three H_2O solvate molecules were located.

The cores of complexes **2** and **3** are very similar. In Fig. 5, ORTEP diagrams of their cores are given. There are two distinct differences between complexes **2** and **3**, however. Complexes **2** and **3** differ in the positioning of the four H_2O and 16 carboxylate ligands. Complex **2** has two H_2O ligands on the Mn(5) atom and one H_2O each on the Mn(7) and Mn(7A) atoms. Complex **3** has two H_2O ligands on the Mn(11) atom and one H_2O each on the Mn(12) and Mn(9) atoms. A key structural difference between complexes **2** and **3** is found in the orientation of the Jahn–Teller (JT) elongation axis of each Mn^{III} ion. As shown in Fig. 5 (top), all of the JT elongation axes in the hydrate complex **3** are roughly parallel and perpendicular to the plane of the disc-like $Mn_{12}O_{12}$ core. For complex **2** in Fig. 5 (bottom), however, it can be seen that one JT axis is abnormally oriented; the situation is slightly complicated by the fact that the molecule has a crystallographic C_2 axis disordering the JT axis about two positions (shown with dashed lines in Fig. 5) but, nevertheless, the JT axis is clearly not in its normal position but in an abnormal position containing a core O^{2-} ion.

3.4. Origin of two out-of-phase ac susceptibility peaks

Chudnovsky and Tejada [41] discussed the mechanism of resonant magnetization tunneling for a SMM such as complex **1**. It was assumed that the magnetization tunneling occurs as a result of a transverse mag-

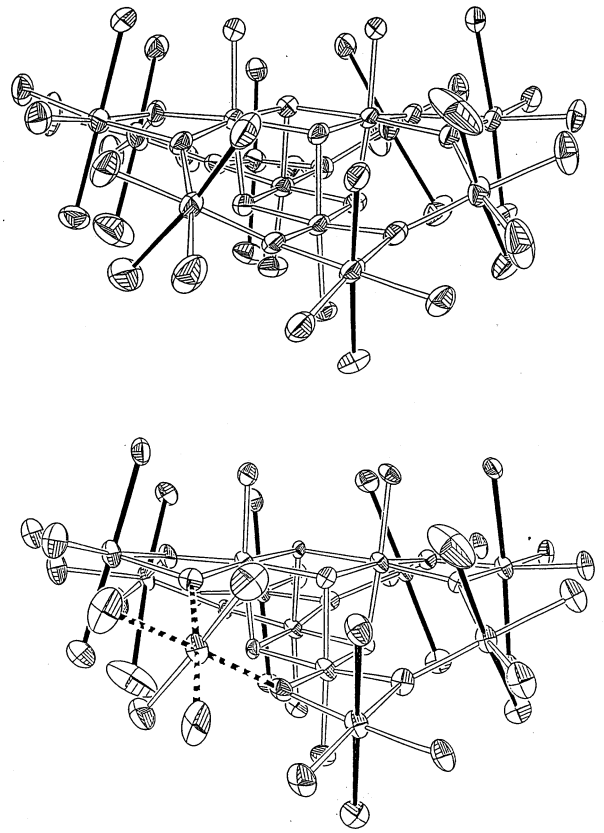

Fig. 5. ORTEP representations of the side views of the cores of (top) $[Mn_{12}O_{12}(O_2CC_6H_4\text{-}p\text{-}Me)_{16}(H_2O)_4]\cdot 3H_2O$ (complex **3**) and (bottom) $[Mn_{12}O_{12}(O_2CC_6H_4\text{-}p\text{-}Me)_{16}(H_2O)_4]\cdot(HO_2CC_6H_4\text{-}p\text{-}Me)$ (complex **2**). The coordination geometries about each Mn atom are shown. Each of the eight Mn^{III} ions show a tetragonally elongated Jahn–Teller distortion. In the case of complex **3** (top) these JT elongation axes are indicated as solid lines. For complex **2** the JT elongation axis dashed lines is pointed at an O^{2-} ion and is unusual. There are two dashed lines because the molecule has a crystallographic C_2 axis disorder.

netic field and the rates of tunneling between pairs of $+m_s$ and $-m_s$ states were calculated. It was concluded that the rate of tunneling for the $m_s = -10$ to $m_s = +10$ conversion of a $S = 10$ molecule occurs with a lifetime longer than the universe when the transverse magnetic field is small. The rate calculated for the $m_s = -3$ to $m_s = +3$ tunneling (see Fig. 1) was found to be close to the experimental value. It was suggested that at low temperatures where steps are seen on hysteresis loops that an individual molecule is excited by a phonon in an Orbach process from the $m_s = -10$ level successively to the $m_s = -9, -8, -7, -6, -5, -4$, and finally the $m_s = -3$ level. After it is excited to the $m_s = -3$ level, the Mn_{12} molecule then tunnels to the $m_s = +3$ level and then it quickly relaxes to the $m_s = +10$ level. A single tunneling channel ($m_s = -3$ to $m_s = +3$) would be opened up and this gives the first step at zero external field in the hysteresis loop.

In addition to a transverse magnetic field, it has now been shown [42] that other interactions, such as a transverse quartic zero-field interaction, are probably also important in influencing the rate of magnetization tunneling. For each Mn_{12} molecule the spin Hamiltonian given in Eq. (2) applies:

$$\hat{H} = \hat{H}_A + \hat{H}_Z + \hat{H}_{sp} + \hat{H}_T \quad (2)$$

The first term $\hat{H}_A$ is for the axial (longitudinal) zero-field interactions, the leading terms of which are given as

$$\hat{H}_A = D\hat{S}_Z^2 - B\hat{S}_Z^4 \quad (3)$$

The parameter D is considerably larger than B and gauges the second-order axial zero-field splitting. The second term in Eq. (2), $\hat{H}_Z$, is just the Zeeman term, which in its simplest form is given in Eq. (4).

$$\hat{H}_Z = g\mu_B\hat{H}_Z\cdot\hat{S}_Z \quad (4)$$

The term $\hat{H}_{sp}$ represents the spin-phonon coupling, where a given Mn_{12} complex interacts with phonons in the crystal. The last term $\hat{H}_T$, representing transverse interactions, is the most important in terms of the rate of magnetization tunneling. Some of the larger terms in $\hat{H}_T$ are given in Eq. (5):

$$\hat{H}_T = g\mu_B\hat{H}_x\cdot\hat{S}_x + E(\hat{S}_x^2 - \hat{S}_y^2) - B_4(\hat{S}_+^4 + \hat{S}_-^4) \quad (5)$$

The raising and lowering operators are given as $\hat{S}_\pm = \hat{S}_x \pm i\hat{S}_y$. The transverse magnetic field $\hat{H}_x$, the rhombic zero-field operator $(\hat{S}_x^2 - \hat{S}_y^2)$ and the quartic zero-field operator $(\hat{S}_+^4 + \hat{S}_-^4)$ mix together the m_s wavefunctions and this facilitates tunneling of the magnetization. There is still considerable research needed to understand this tunneling phenomenon [43].

The Mn_{12}–acetate complex **1** is excited by phonons to an $m_s = -3$ tunneling channel. Tunneling of the magnetization in the ground state levels ($m_s = \pm 10$) has not been observed for complex **1**. Tunneling from the lowest energy level has been observed for two other single-molecule magnets. The complex $[Mn_4O_3Cl(O_2CMe)_3(dbm)_3]$ (**4**) where dbm^- is the monoanion of dibenzoylmethane, has an $S = 9/2$ ground state [44]. Since complex **4** shows frequency-dependent out-of-phase ac susceptibility signals and magnetization hysteresis loops below 0.90 K, this complex is a SMM. Steps are seen on each hysteresis loop. An Arrhenius plot of the magnetization relaxation data for complex **4** indicates a thermally activated region between 2.0 and 0.70 K and a temperature-independent region at temperatures below 0.70 K. A fit of the data in the temperature-dependent region gives $U_{eff} = 11.8$ K and $\tau_0 = 3.6 \times 10^{-7}$ s. With the D-value obtained from HFEPR data for this $S = 9/2$ complex **4**, U can be calculated as 15.2 K ($= 10.6$ cm^{-1}). It was concluded [44] that the temperature-independent magnetization relaxation must correspond to magnetization tunneling between the lowest degenerate levels, the $m_s = 9/2$ and $-9/2$ levels for the $S = 9/2$ complex **4**. A temperature-

independent magnetization relaxation below 0.35 K has also been reported for a Fe_8^{III} complex with the formula $[Fe_8O_2(OH)_{12}(tacn)_6]Br_8$ (complex **5**) that has an $S = 10$ ground state [45]. Complex **5** has been found to have $U_{eff} = 24.5$ K and zero-field interaction parameters of $D = -0.27$ K and $E = -0.046$ K. Tunneling in the lowest energy $m_s = \pm 10$ levels is seen for this Fe_8^{III} complex.

It is important to note that Mn_4 complex **4** and Fe_8 complex **5** show larger rates of tunneling in the lowest-energy level than does the Mn_{12}–acetate complex **1** because they possess relatively large transverse interactions, i.e. $\hat{H}_T$ terms in Eq. (5). Due to its crystal site symmetry the Mn_{12}–acetate complex **1** has no rhombic zero-field splitting ($E = 0$). Complexes **4** and **5** probably show tunneling in the lowest-energy levels because each of these complexes is of lower symmetry and this gives a non-zero E value. Tunneling is not totally due to rhombic zero-field interactions for it has been shown that transverse magnetic fields are also important. The magnetic field can result from an external magnetic field or there could be an internal field in the crystal from neighboring molecules. In fact, a transverse component of the magnetic field created by the nuclear spins within the molecule is also important [44,46,47].

Complex **2** shows its out-of-phase ac susceptibility signals at essentially one-half the temperature for the peaks for complex **3**. For complex **2** it is found that $U_{eff} = 38$ K, whereas complex **3** has been evaluated to have $U_{eff} = 64$ K. Complex **3** behaves similarly to the high-symmetry Mn_{12}–acetate complex **1**. As described above, complex **3** has all of its Mn^{III} JT distortion axes oriented nearly parallel, as in complex **1**. In contrast, the JT distortion axis at one Mn^{III} ion in complex **2** is found to be tipped approximately 90° from the other axes and complex **2** thus has a lower symmetry than complex **3**. It is likely that the rhombic zero-field interactions in complex **2** are significantly larger than those in complex **3** and this means that the tunneling matrix elements for complex **2** are larger than those for complex **3**. As a consequence, complex **2** may well have a different tunneling channel than complex **3**. Complex **3** behaves similarly to complex **1** and therefore has an $m_s = -3$ to $m_s = +3$ tunneling channel. It could be suggested that complex **2** has a lower energy tunneling channel, such as an $m_s = -5$ to $m_s = +5$ channel, or at least a much faster rate of magnetization tunneling.

It is unlikely that the difference in magnetization relaxation rates between complexes **2** and **3** is due to very different potential-energy barriers, i.e. values of U. The axial zero-field splitting parameters (D values) are similar for the two complexes, as indicated by the steps in the hysteresis loops; the increments between steps are essentially the same for the two isomers. The analysis of variable-field dc magnetization data for complex **2** indicates that it might have an $S = 9$ ground state, whereas complex **3** has an $S = 10$ ground state. This would have to be confirmed by HFEPR data. A change in ground state spin from $S = 10$ to $S = 9$ without a change in D would only lead to a decrease of 19% in the height of the potential-energy barrier shown in Fig. 1. It is suspected that the rate of magnetization tunneling in complex **2** is appreciably greater than in complex **3** primarily because the rhombic zero-field interactions are much greater in complex **2**. Very detailed HFEPR or inelastic neutron scattering experiments are now required to evaluate the precise magnitude of the rhombic zero-field interactions in these complexes.

Acknowledgements

D.N.H and G.C. thank the National Science Foundation for support of this research.

References

[1] T. Lis, Acta Crystallogr., Sect. B 36 (1980) 2042.
[2] P.D.W. Boyd, Q. Li, J.B. Vincent, K. Folting, H.-R. Chang, W.E. Streib, J.C. Huffman, G. Christou, D.N. Hendrickson, J. Am. Chem. Soc. 110 (1988) 8537.
[3] A. Caneschi, D. Gatteschi, R. Sessoli, A.L. Barra, L.C. Brunel, M. Guillot, J. Am. Chem. Soc. 113 (1991) 5873.
[4] A.R. Schake, H.-L. Tsai, N. de Vries, R.J. Webb, K. Folting, D.N. Hendrickson, G. Christou, J. Chem. Soc. Chem., Commun. (1992) 181.
[5] R. Sessoli, H.-L. Tsai, A.R. Schake, S. Wang, J.B. Vincent, K. Folting, D. Gatteschi, G. Christou, D.N. Hendrickson, J. Am. Chem. Soc. 115 (1993) 1804.
[6] R. Sessoli, D. Gatteschi, A. Caneschi, M.A. Novak, Nature 365 (1993) 141.
[7] D. Gatteschi, A. Caneschi, L. Pardi, R. Sessoli, Science 265 (1994) 1054.
[8] J. Villain, F. Hartman-Boutron, R. Sessoli, A. Rettori, Europhys. Lett. 27 (1994) 159.
[9] J.J. Eppley, H.-L. Tsai, N. De Vries, K. Folting, G. Christou, D.N. Hendrickson, J. Am. Chem. Soc. 117 (1995) 301.
[10] A.L. Barra, A. Caneschi, D. Gatteschi, R. Sessoli, J. Am. Chem. Soc. 117 (1995) 8855.
[11] M.A. Novak, R. Sessoli, A. Caneschi, D. Gatteschi, J. Magn. Magn. Mat. 146 (1995) 211.
[12] B. Barbara, W. Wernsdorfer, L.C. Sampaio, J.G. Park, C. Paulsen, M.A. Novak, R. Ferré, D. Mailly, R. Sessoli, A. Caneschi, K. Hasselbach, A. Benoit, L.J. Thomas, Magn. Magn. Mat. 140-144 (1995) 1825.
[13] H.J. Eppley, S. Wang, H.-L. Tsai, S.M. Aubin, K. Folting, W.E. Streib, D.N. Hendrickson, G. Christou, Mol. Cryst. Liq. Cryst. 274 (1995) 159.
[14] H.-L. Tsai, H.J. Eppley, N. de Vries, K. Folting, G. Christou, D.N. Hendrickson, Mol. Cryst. Liq. Cryst. 274 (1995) 167.
[15] M.A. Novak, R. Sessoli, in: L. Gunther, B. Barbara (Eds.), Quantum Tunneling of Magnetization — QTM'94, Kluwer Academic Publishers, Dordrecht, 1995, pp. 171–188.
[16] C. Paulsen, J.-G. Park, in: L. Gunther, B. Barbara (Eds.), Quantum Tunneling of Magnetization — QTM'94, Kluwer Academic Publishers, Dordrecht, 1995, pp. 189–207.

[17] C. Paulsen, J.-G. Park, B. Barbara, R. Sessoli, A.J. Caneschi, Magn. Magn. Mat. 140-144 (1995) 379.
[18] C. Paulsen, J.G. Park, B. Barbara, R. Sessoli, A. Caneschi, J. Magn. Magn. Mat. 140-144 (1995) 1891.
[19] R. Politi, A. Rettori, F. Hartmann-Boutron, J. Villain, Phys. Rev. Lett. 75 (1995) 537.
[20] J.R. Friedman, M.P. Sarachik, J. Tejada, J. Maciejewski, R.J. Ziolo, Appl. Phys. 79 (1996) 6031.
[21] J.R. Friedman, M.P. Sarachik, J. Tejada, R. Ziolo, Phys. Rev. Lett. 76 (1996) 3830.
[22] L. Thomas, F. Lionti, R. Ballou, D. Gatteschi, R. Sessoli, B. Barbara, Nature 383 (1996) 145.
[23] J. Tejada, R.F. Ziolo, X.X. Zhang, Chem. Mater. 8 (1996) 1784.
[24] J.M. Hernandez, X.X. Zhang, F. Luis, J. Bartolomé, J. Tejada, R. Ziolo, Europhys. Lett. 35 (1996) 301.
[25] E.M. Chudnovsky, Science 274 (1996) 938.
[26] P.A. Reynolds, E.P. Gilbert, B.N. Figgis, Inorg. Chem. 35 (1996) 545.
[27] D. Gatteschi, Curr. Opin. Solid State Mater. Sci. 1 (1996) 192.
[28] A.L. Burin, N.V. Prokof'ev, P.C.E. Stamp, Phys. Rev. Lett. 76 (1996) 3040.
[29] P. Politi, A. Rettori, F. Harmann-Boutron, J. Villain, Phys. Rev. Lett. 76 (1996) 3041.
[30] B. Schwarzschild, Physics Today (1997) January 17.
[31] F. Lionti, L. Thomas, R. Ballou, B. Barbara, A. Sulpice, R. Sessoli, D. Gatteschi, J. Appl. Phys. 81 (1997) 4608.
[32] J.R. Friedman, M.P. Sarachik, J.M. Hernandez, X.X. Zhang, J. Tejada, E. Molins, R. Ziolo, J. Appl. Phys. 81 (1997) 3978.
[33] S.M.J. Aubin, S. Spagna, H.J. Eppley, R.E. Sager, K. Folting, G. Christou, D.N. Hendrickson, Mol. Cryst. Liq. Cryst. (in press).
[34] H.J. Eppley, S.M.J. Aubin, M.W. Wemple, D.M. Adams, H.-L. Tsai, V.A. Grillo, S.L. Castro, Z. Sun, K. Folting, J.C. Huffman, D.N. Hendrickson, G. Christou, Mol. Cryst. Liq. Cryst. 305 (1997) 167.
[35] A.L. Barra, D. Gatteschi, R. Sessoli, Phys. Rev. B 56 (1997) 8192.
[36] F. Luis, J. Bartolomé, J.F. Fernández, J. Tejada, J.M. Hernández, X.X. Zhang, R. Ziolo, Phys. Rev. B 55 (1997) 11448.
[37] J.M. Hernandez, X.X. Zhang, F. Luis, J. Tejada, J.R. Friedman, M.P. Sarachik, R. Ziolo, Phys. Rev. B 55 (1997) 5858.
[38] Z. Sun, D, Ruiz, N.R. Dilley, M. Soler, J. Ribas, I.A. Guzei, A.L. Rheingold, K. Folting, M.B. Maple, G. Christou, D.N. Hendrickson, Chem. Commun. (1999) 1973.
[39] T. Sala, M.V. Sargent, J. Chem. Soc., Chem. Commun. (1978) 253.
[40] E.A. Boudreaux, L.N. Mulay (Eds.), Theory and Applications of Molecular Paramagnetism, J. Wiley & Sons, New York, 1976.
[41] E.M. Chudnovsky, J. Tejada, Macroscopic Quantum Tunneling of the Magnetic Moment, Cambridge University Press, Cambridge, 1998.
[42] A. Caneschi, D. Gatteschi, C. Sangregorio, R. Sessoli, L. Sorace, A. Cornia, M.A. Novak, C. Paulsen, W.J. Wernsdorfer, Magn. Magn. Mater. 200 (1999) 182.
[43] A.D. Kent, Y. Zhong, L. Bokacheva, D. Ruiz, D.N. Hendrickson, Europhys. Lett. 49 (2000) 521.
[44] S.M.J. Aubin, N.R. Dilley, L. Pardi, J. Krzystek, M.W. Wemple, L.-C. Brunel, M.B. Maple, G. Christou, D.N. Hendrickson, J. Am. Chem. Soc. 120 (1998) 4991.
[45] C. Sangregorio, T. Ohm, C. Paulsen, R. Sessoli, D. Gatteschi, Phys. Rev. Lett. 78 (1997) 4645.
[46] S.M.J. Aubin, S. Spagna, H.J. Eppley, R.E. Sager, G. Christou, D.N. Hendrickson, Chem. Commun. (1998) 803.
[47] W. Wernsdorfer, A. Caneschi, R. Sessoli, D. Gatteschi, A. Cornia, V. Villar, C. Paulsen, Phys. Rev. Lett. 84 (2000) 2965.